



Since January 2020 Elsevier has created a COVID-19 resource centre with free information in English and Mandarin on the novel coronavirus COVID-19. The COVID-19 resource centre is hosted on Elsevier Connect, the company's public news and information website.

Elsevier hereby grants permission to make all its COVID-19-related research that is available on the COVID-19 resource centre - including this research content - immediately available in PubMed Central and other publicly funded repositories, such as the WHO COVID database with rights for unrestricted research re-use and analyses in any form or by any means with acknowledgement of the original source. These permissions are granted for free by Elsevier for as long as the COVID-19 resource centre remains active.



## Cardiothoracic Imaging

## Early prediction of severity in coronavirus disease (COVID-19) using quantitative CT imaging

Kunwei Li<sup>a,b,1</sup>, Xueguo Liu<sup>a,b,1</sup>, Rowena Yip<sup>c</sup>, David F. Yankelevitz<sup>c</sup>, Claudia I. Henschke<sup>c</sup>, Yayuan Geng<sup>d</sup>, Yijie Fang<sup>a</sup>, Wenjuan Li<sup>a</sup>, Cunxue Pan<sup>a</sup>, Xiaojun Chen<sup>a</sup>, Peixin Qin<sup>a</sup>, Yinghua Zhong<sup>a</sup>, Kunfeng Liu<sup>a</sup>, Shaolin Li<sup>a,b,\*</sup>

<sup>a</sup> Department of Radiology, Fifth Affiliated Hospital of Sun Yat-sen University, 52 East Meihua Road, Zhuhai 519000, China

<sup>b</sup> Guangdong Provincial Key Laboratory of Biomedical Imaging, Fifth Affiliated Hospital of Sun Yat-sen University, 52 East Meihua Road, Zhuhai 519000, China

<sup>c</sup> Department of Radiology, Icahn School of Medicine at Mount Sinai, 1 Gustave Levy Place, New York, NY 10029, United States of America

<sup>d</sup> Huiying Medical Technology Co., Ltd, Room A206, B2, Dongsheng Science and Technology Park, HaiDian District, Beijing 100192, China

## ARTICLE INFO

## Keywords:

COVID-19

Prognosis

Tomography, X-ray computed

Quantitative evaluation

Deep learning

## ABSTRACT

**Purpose:** To evaluate whether the extent of COVID-19 pneumonia on CT scans using quantitative CT imaging obtained early in the illness can predict its future severity.

**Methods:** We conducted a retrospective single-center study on confirmed COVID-19 patients between January 18, 2020 and March 5, 2020. A quantitative AI algorithm was used to evaluate each patient's CT scan to determine the proportion of the lungs with pneumonia (VR) and the rate of change (RAR) in VR from scan to scan. Patients were classified as being in the severe or non-severe group based on their final symptoms. Penalized B-splines regression modeling was used to examine the relationship between mean VR and days from onset of symptoms in the two groups, with 95% and 99% confidence intervals.

**Results:** Median VR max was 18.6% (IQR 9.1–32.7%) in 21 patients in the severe group, significantly higher ( $P < 0.0001$ ) than in the 53 patients in non-severe group (1.8% (IQR 0.4–5.7%)). RAR was increasing with a median RAR of 2.1% (IQR 0.4–5.5%) in severe and 0.4% (IQR 0.1–0.9%) in non-severe group, which was significantly different ( $P < 0.0001$ ). Penalized B-spline analyses showed positive relationships between VR and days from onset of symptom. The 95% confidence limits of the predicted means for the two groups diverged 5 days after the onset of initial symptoms with a threshold of 11.9%.

**Conclusion:** Five days after the initial onset of symptoms, CT could predict the patients who later developed severe symptoms with 95% confidence.

## 1. Introduction

Coronavirus disease 2019 (COVID-19) has rapidly increased in prevalence to become a global pandemic by March 2020.<sup>1</sup> It is caused by the severe acute respiratory syndrome coronavirus 2 (SARS-CoV-2). In the United States, most professional organizations and societies recommend against the use of CT scanning for diagnostic evaluation even though it is accepted that CT findings can precede positive findings on reverse transcriptase polymerase chain reaction testing (RT-PCR).<sup>2</sup>

Early in the course of the pandemic, an editorial described the use of CT for diagnostic purposes as “a distraction” and “possibly dangerous”.<sup>3</sup> In addition, the utilization of CT will increase the risk of radiation exposure to the patient, risk of COVID-19 transmission to uninfected health people, and the consumption of personal protection equipment and downtime of CT scanning rooms. However, both for diagnostic purposes and also for follow-up, other countries, notably China, routinely obtain CT scans on all proven positive cases.<sup>4</sup> The radiologic features of COVID-19 have been well described and include features similar to those found in

\* Corresponding author at: Department of Radiology, Fifth Affiliated Hospital of Sun Yat-sen University, Zhuhai 519000, China; Guangdong Provincial Key Laboratory of Biomedical Imaging, Fifth Affiliated Hospital of Sun Yat-sen University, Zhuhai 519000, China.

E-mail addresses: [likunwei@mail.sysu.edu.cn](mailto:likunwei@mail.sysu.edu.cn) (K. Li), [liuxueguo@mail.sysu.edu.cn](mailto:liuxueguo@mail.sysu.edu.cn) (X. Liu), [rowena.yip@mountsinai.org](mailto:rowena.yip@mountsinai.org) (R. Yip), [david.yankelevitz@mountsinai.org](mailto:david.yankelevitz@mountsinai.org) (D.F. Yankelevitz), [claudia.ihenschke@mountsinai.org](mailto:claudia.ihenschke@mountsinai.org) (C.I. Henschke), [gengyayuan@huiyihuiying.com](mailto:gengyayuan@huiyihuiying.com) (Y. Geng), [fangyj5@mail.sysu.edu.cn](mailto:fangyj5@mail.sysu.edu.cn) (Y. Fang), [liwj48@mail2.sysu.edu.cn](mailto:liwj48@mail2.sysu.edu.cn) (W. Li), [chenxjun5@mail.sysu.edu.cn](mailto:chenxjun5@mail.sysu.edu.cn) (X. Chen), [liukf6@mail2.sysu.edu.cn](mailto:liukf6@mail2.sysu.edu.cn) (K. Liu), [lishlin5@mail.sysu.edu.cn](mailto:lishlin5@mail.sysu.edu.cn) (S. Li).

<sup>1</sup> Kunwei Li and Xueguo Liu have equal contributions to the study.

<https://doi.org/10.1016/j.clinimag.2021.02.003>

Received 17 June 2020; Received in revised form 21 January 2021; Accepted 2 February 2021

Available online 10 February 2021

0899-7071/© 2021 Elsevier Inc. All rights reserved.

organizing pneumonia with peripheral ground glass opacities (GGOs) that are bilateral, multi-lobar, nodular and mass-like with a basilar predilection.<sup>5</sup> There are also many additional, more non-specific features.<sup>6</sup>

The general time course for the radiologic findings of COVID-19 has been described.<sup>7,8,9</sup> GGOs can usually be found within the first 4–5 days of initial symptom presentation and peak between 6 and 13 days. In China, four categories of severity of COVID-19 disease have also been described in the Diagnosis and Treatment Plan of COVID-19 issued by National Health Commission (7th ed.).<sup>9</sup> The four categories are: [1] *mild type* defined as having mild clinical symptoms without pneumonia in imaging; [2] *common type* defined by having fever, respiratory tract and other symptoms, pneumonia on imaging; [3] *severe type* defined as having respiratory distress, respiratory rate  $\geq 30$  times/min, oxygen saturation  $\leq 93\%$ , PaO<sub>2</sub>/FiO<sub>2</sub>  $\leq 300$  mm Hg; [4] *critical type* defined by respiratory failure requiring mechanical ventilation, shock, other organ failure, ICU monitoring and treatment.

In managing patients with COVID-19, the ability to predict in the first few days after onset of symptoms which patients will ultimately progress into the severe or critical category would be highly useful for management and planning purposes. It would allow for planning on the likelihood of more intensive treatment, possibly assisted ventilation and similarly, who will likely need only minor supportive care. Based on the use of CT scans of patients with confirmed COVID-19 diagnosis, the goal was to evaluate the extent to which early quantitative CT findings are useful to predict the extent of disease progression prior to reaching the severe stage.

## 2. Methods

### 2.1. Case selection

A retrospective, single-center study was performed of SARS-CoV-2 laboratory-confirmed patients between January 18, 2020 and March 5, 2020 in Zhuhai, China. A patient was confirmed as positive by high-throughput sequencing or real-time RT-PCR assay<sup>10</sup> (Shanghai Zhijiang Biotechnology Co. Shanghai, China) and confirmed by the Centers for Disease Control. This study was approved by the institutional review board of the fifth hospital of Sun Yat-sen university and requirement for informed consent was waived. CT imaging features in some patients included in this study have been previously reported<sup>5,8,11</sup> but not on AI quantitative CT parameters presented here.

Inclusion criteria were patients with: (a) positive new coronavirus nucleic acid antibody; (b) age  $\geq 14$ ; (c)  $\geq 2$  consecutive thin-section CT scans within seven days; (d) clinical symptoms of COVID-19; and (e) pneumonia on at least one CT examination. Only patients who met all inclusion criteria listed above were included in this study. Patients with CT scans with obvious alternative diagnoses were excluded. Symptoms were obtained by chart review.

COVID-19 disease severity categories of [2-common], [3-severe], and [4-critical] were aggregated into two at discharge according to the most severe category at any time during their admission: the *non-severe group* which included all patients with COVID-19 category [2-common] and the *severe group* which included all patients who developed COVID-19 categories [3-severe] and [4-critical].

### 2.2. CT protocol

All scans were performed with patients in the supine position during end-inspiration without intravenous contrast on three CT scanners, uCT 760, uMI 780 scanners (United Imaging; Shanghai, China) and Precision 32 (CAMPO Imaging; Shenyang, China). Images were obtained from the apex to lung bases. Scans were obtained using a standard dose protocol, reconstructed at 1.0 mm/1.1 mm slice thickness with 0.7 mm increment, 512 mm  $\times$  512 mm matrix and a sharp reconstruction kernel. Lung window width and level settings were 1500 Hounsfield units (HU) and

–600 HU.

### 2.3. CT image review

A deep learning-based algorithm (HY Medical Technology) trained on annotated datasets of COVID-19 was used to segment and quantify the total volume of both lungs (TV) and the total volume of the lesions presumed to represent COVID-19 pneumonia (e.g., GGOs, consolidation) (DV) for each patient. Detailed information about the deep learning algorithm and structure has been previously described.<sup>12,13</sup>

The determination of TV and DV was made using the software and accuracy was reviewed by two radiologists with 5- and 3-years of experience Y.F and W.L. In cases where the software failed to provide the TV and DV estimates, estimates were visually estimated by a third radiologist with 17 years of experience K.L.

For each patient, the following values were calculated for each CT scans using the quantitative parameters (TV and DV) derived from the AI assessments:

1. Volume Ratio (VR) = DV/TV, the ratio of CT volume of all infected lung regions to the whole lung volume.
2. Ratio Alteration Rate (RAR) = (VR<sub>2</sub> – VR<sub>1</sub>) / days, the change in VR from time<sub>1</sub> (VR<sub>1</sub>) to time<sub>2</sub> (VR<sub>2</sub>), divided by days between the two CT scans.
3. Maximum volume ratio (VR<sub>max</sub>) was the highest VR attained among all CT scans for the particular patient and the day it was reached was D<sub>max</sub>.

We defined two disease phases based on the CT scans, the progressive and recovery phases. For each patient, the CT scan was classified as:

Being in the progressive phase, if VR  $\leq$  VR<sub>max</sub>, RAR was positive, and the date of the CT scan was on or before D<sub>max</sub> and

Being in the recovery phase: if VR < VR<sub>max</sub>, RAR was negative, and the date of the CT scan was after D<sub>max</sub>.

Among the 74 patients who met the study criteria, 21 in the severe group and 53 in the non-severe group, there were a total of 305 CT scans. Radiologists identified AI errors in 26 CT scans, 25 in the non-severe group and one in the severe group. False positive AI results were identified in four CT scans (all non-severe), due to the AI algorithm incorrectly identifying dependent atelectasis as pneumonia. False negative AI results were found in 22 CT scans (21 non-severe, 1 severe) due to the AI algorithm failing to detect very faint or very small subtle lesions. For these 26 CT scans, VR was estimated: 1) for the four false positive CT scans, VR was set at 0% as there were no lesions; 2) for the 22 false negative CT scans, the senior radiologist K.L. visually estimated the highest value for VR, using comparable CT scans with detectable lesion volume as a reference.

### 2.4. Statistical analysis

Categorical variables were summarized as percentages. Continuous variables were summarized as means  $\pm$  standard deviations (SD) or as medians and interquartile-ranges (IQR). Differences were evaluated with Student's t or Mann-Whitney U test for continuous variables and with Chi-square or Fisher's exact tests for categorical variables. Median VR and RAR at progressive and recovery phases were calculated for each patient in severe and non-severe groups. VR<sub>max</sub> and RAR for each group were compared using Wilcoxon test.

We examined the differences in VR between groups during the progressive phase. Mean response of VR versus time were calculated and penalized B-splines using corrected Akaike's Information Criterion (AICC) were fitted, separately for each group. 95% and 99% confidence intervals for the predicted mean of VR were computed. Statistical analysis was performed using SPSS V25.0 (IBM Corp., Armonk, NY) and

SAS v9.4 (Cary, NC).

### 3. Results

#### 3.1. Demographic and clinical characteristics

Our patient cohort came from Zhuhai, Guangdong, a coastal city in southern China, near Macau and Hong Kong. Patient demographics and comorbidities are described in Table 1. For the 74 patients, 21 in the severe group and 53 in the non-severe group, the first chest CT was obtained on average 4.8 days (SD: 4.2, range: 0–19 days) after the onset of initial symptoms. Each patient had an average of 4.1 (SD: 1.4) CT scans (range: 1–8) with a mean interval of 5.0 (SD: 5.0) days (range: 0–26.0 days) between the scans. Preexisting conditions were more prevalent among the 21 patients in the severe group compared to the 53 patients in the non-severe group (48% vs. 36%,  $P = 0.35$ ), however, the difference did not reach statistical significance. For the 21 patients who developed severe disease, average number of days from onset of initial symptoms to severe symptoms was 8.9 (SD: 3.9, range: 0–17 days).

**Table 1**  
Characteristics of the patient cohort.<sup>a</sup>

Characteristics	Severe (n = 21)	Non-severe (n = 53)	P value
Age (years)			0.005
Mean ± SD	58 ± 13	47 ± 15	
Range	32–80	15–75	
Gender			0.17
Male	12 (57)	21 (40)	
Female	9 (43)	32 (60)	
Epidemiological history			0.35
Recent travel to Hubei	15 (72)	45 (85)	
Exposure to infected people	3 (14)	5 (9)	
Unknown exposure	3 (14)	3 (6)	
Smoking history			0.34
Smoker	3 (14)	3 (6)	
Never smoker	18 (86)	50 (94)	
Comorbidities			
Any	10 (48)	19 (36)	0.35
Hypertension	6 (29)	11 (21)	0.54
Diabetes	4 (19)	2 (4)	0.05
Hyperlipidemia	3 (14)	2 (4)	0.13
Pulmonary disease <sup>b</sup>	2 (10)	0 (0)	0.08
Cerebrovascular disease	0 (0)	1 (2)	1.00
Coronary heart disease	0 (0)	1 (2)	1.00
Cured cancers <sup>c</sup>	1 (5)	1 (2)	0.49
Mental disease	0 (0)	2 (4)	1.00
Other <sup>d</sup>	0 (0)	4 (8)	0.57
Initial symptoms			
Any	20 (95)	52 (98)	0.49
Fever	17 (81)	34 (64)	0.16
Low grade fever (37.3–38.0)			
Moderate grade fever (38.1–39.0)			
Cough	10 (48)	36 (68)	0.10
Expectoration	0 (0)	19 (36)	0.001
Throat pain	4 (19)	6 (11)	0.62
Dyspnea	0 (0)	1 (2)	1.00
Nasal congestion and runny nose	1 (5)	7 (13)	0.52
Headache and dizziness	2 (10)	3 (6)	0.62
Fatigue	6 (29)	2 (4)	0.007
Muscle soreness	4 (19)	5 (9)	0.46
Diarrhea	2 (10)	2 (4)	0.32
Nausea and vomiting	0 (0)	3 (6)	0.55
The period between the onset and admission (day) (median (IQR))	3 (1.3–6.0)	4 (1.0–6.8)	0.87

Each cell indicates the number (percentage) of patients in the corresponding disease status (severe, non-severe).

<sup>a</sup> Our patient cohort came from Zhuhai, Guangdong, a coastal city in southern China, near Macau and Hong Kong.

<sup>b</sup> Pulmonary disease includes tuberculosis and bronchiectasis.

<sup>c</sup> Cured cancers include thyroid cancer and bladder cancer.

<sup>d</sup> Other comorbidities include one thigh mass; one anemia, one hypothyroidism, one hepatitis B.

The median number of days from the onset of symptoms to  $D_{max}$  (the day VR reached a maximum value for any particular patient) was 11 (IQR 9–13) days for patients in severe group and 10 (IQR 7–13) days for patient in non-severe group which was not significantly different ( $P = 0.52$ ).

Of the 305 CT scans on these 74 patients, 173 were obtained during the progressive phase and 132 during the recovery phase. The median number of days from onset of symptoms to CT was 7 (IQR 4–11) days (range: 0–22 days) in the progressive phase and 20 (IQR 15–28) days (range: 5–54 days) in recovery phase.

#### 3.2. VR, $VR_{max}$ and RAR in severe and non-severe groups

Median  $VR_{max}$  was 18.6% (IQR 9.1–32.7%) in severe group, which was significantly higher ( $P < 0.0001$ ) than that in non-severe group, which was 1.8% (IQR 0.4–5.7%).

The median VR during the progressive phase was 12.0% (IQR 6.3–24.0%) for the 21 patients in the severe group and 1.3% (IQR 0.2–3.7%) for the 53 patients in the non-severe group (Table 2). Median VR at recovery phase was 5.2% (IQR 2.9–15.3%) in severe and 0.6% (IQR 0.1–1.8%) in non-severe group. Whether in the progressive or the recovery phases, the VR in severe group was significantly higher than that in non-severe group (Table 2).

RAR was increasing with a median RAR of 2.1% (IQR 0.4–5%) in severe and 0.4% (IQR 0.1–0.9%) in non-severe group. RAR was decreasing with a median of 0.8% (IQR –1.7 to –0.4%) in severe and 0.1% (IQR –0.4 to –0.03%) in non-severe group. Whether in the progressive or the recovery phases, the RAR in severe group were significantly higher than that in non-severe group (Table 2).

Fig. 1a–b shows the changes in VR for each patient over time after initial onset of symptom, separately for the severe group and non-severe group during the progression of the disease. The plots demonstrate that the rate of change in VR was faster in patients in the severe group compared to those in the non-severe group. While VRs varied between 0.0% and 90% during the progressive phase for the 21 patients with severe disease, none of the 53 patients with non-severe disease had VR more than 25.0% at any time during the progressive phase. In four of the 21 patients with severe disease, however, VRs remained below 10% on CT scans during the entire progressive phase.

Fig. 2 shows the fitted penalized B-splines of mean VR along with their corresponding 95% and 99% confidence intervals for each day after onset of the symptoms, separately for the severe and non-severe groups. Based on visual assessment of the fitted penalized B-splines and confidence bands, although the predicted mean VR at day 0 was higher in the severe group, the slope of the predicted mean curve for the severe group was positive with a greater magnitude compared to the slope for the non-severe group. The 95% confidence intervals for the severe and non-severe groups overlapped in the initial days after onset of the disease. The two 95% confidence bands started to diverge between day 5 and day 6 from the onset of symptoms, the non-overlapping confidence intervals indicate that the mean VR was significantly different between patients with severe disease and patients with non-severe disease after day 5. Penalized spline of the predicted mean

**Table 2**  
Median and interquartile range of VR and RAR in severe and non-severe groups on 74 cases with 305 CT scans.

AI indices	Severe (n = 21)	Non-severe (n = 53)	P value
VR at progressive phase	12.0% (6.3–24.0%)	1.3% (0.2–3.7%)	<0.0001
VR at recovery phase	5.2% (2.9–15.3%)	0.6% (0.1–1.8%)	<0.0001
RAR at progressive phase	2.1% (0.4–5.5%)	0.4% (0.1–0.9%)	0.003
RAR at recovery phase	–0.8% (–1.7 to –0.4%)	–0.1% (–0.4 to –0.03%)	<0.0001

Definition of abbreviations: VR = volume ratio; RAR = ratio alteration rate.

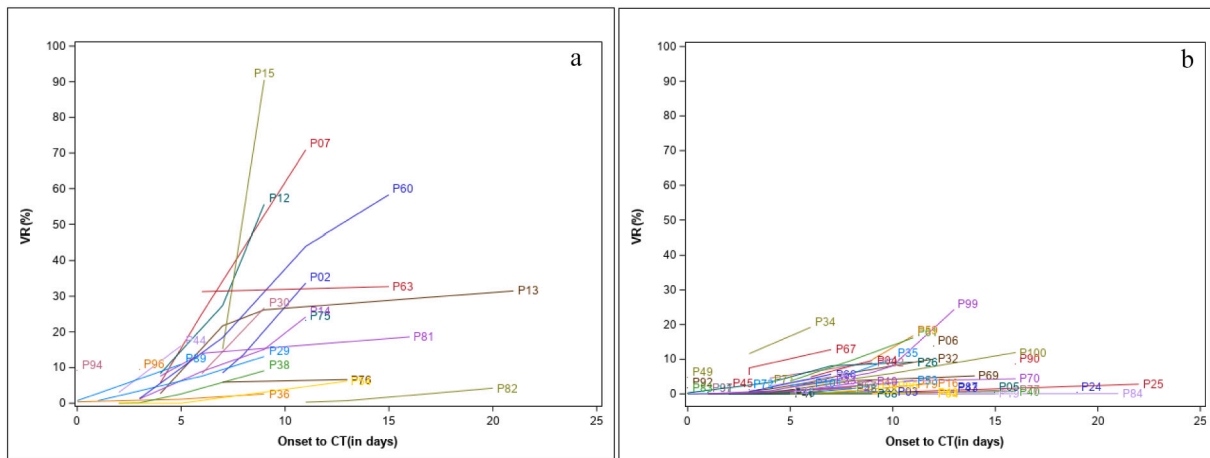


Fig. 1. Change in VR on chest CT from onset of initial symptoms (in days) for (a) the 21 patients with severe disease and (b) the 53 patients with non-severe disease. Each line represents an individual patient.

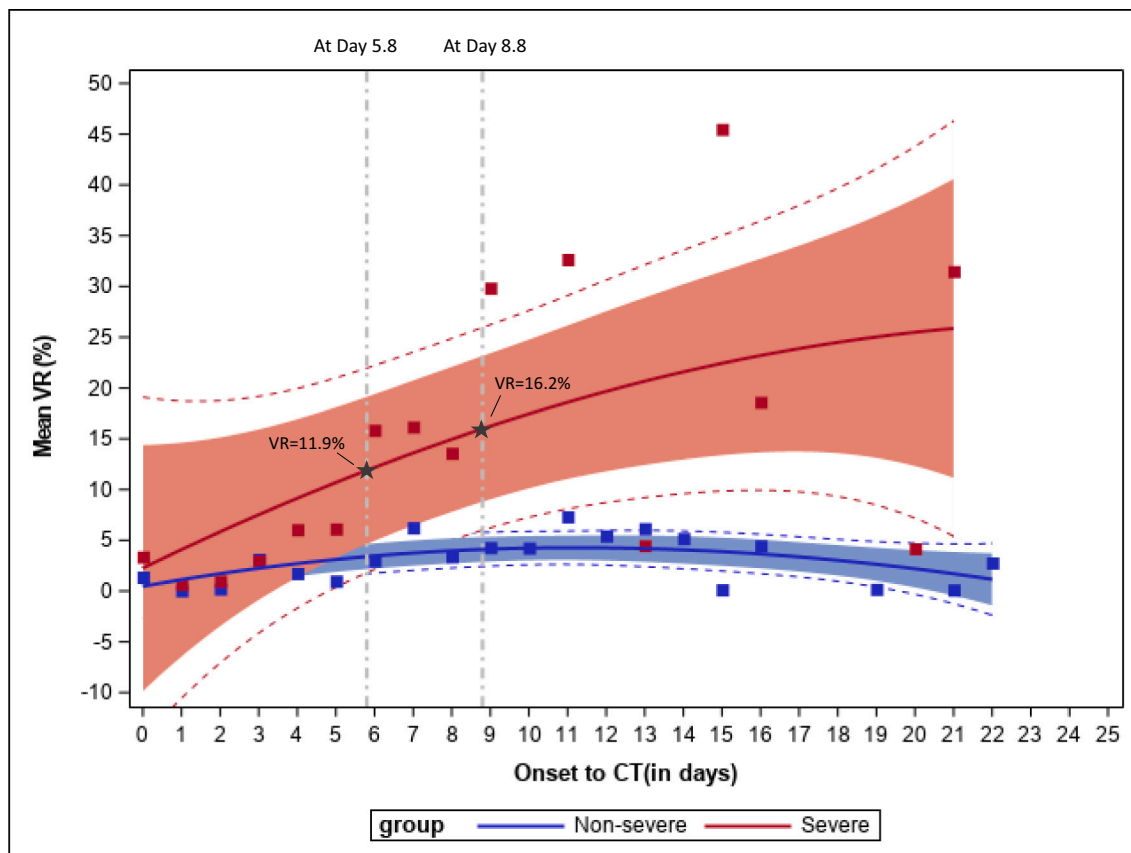


Fig. 2. Mean VR by time from onset of symptoms to CT during the progressive phase of the disease, separately by patients with severe and non-severe disease groups. Mean VRs in the severe group (red) and non-severe (blue) group are indicated by the squares, respectively. Solid lines show predicted mean curve. 95% confidence bands for the two groups are shown for the severe group (in red) and the non-severe group (in blue). Dashed lines outside of the filled area represent the 99% confidence interval. Reference lines were drawn to indicate the point of divergence between the confidence bands for the severe and non-severe groups. Penalized spline for the severe group indicates that a threshold of VR 11.9% can be used to identify patients who are on the course of developing severe disease after day 5.8 with 95% confidence. Similarly, a threshold of VR 16.2% can be used after day 8.8 to achieve 99% confidence. (For interpretation of the references to color in this figure legend, the reader is referred to the web version of this article.)

curve for severe group showed that the predicted mean VR was 11.9% at the point of divergence (day 5.8). Of the 21 patients in the severe group, 18 (85.7%) developed symptoms classified as severe after 5 days, suggesting that CT provided early identification of these patients. The remaining three patients with severe disease developed severe

symptoms at 0, 3 and 5 days.

The 99% confidence bands for the two disease groups diverged 8–9 days after the onset of initial symptoms. At the point of divergence (day 8.8), the predicted mean VR was 16.2% based on the predicted mean curve for severe group. 11 (52.4%) of the 21 patients developed

symptoms being classified as severe after 8 days. These results suggested that for patients with borderline VR values or other concerns 5 days after onset of initial symptoms, a repeat CT in another 3–4 days can be performed to gain additional confidence in evaluating whether the person will progress to severe disease. With the average time to severity being 8.9 days from the onset of initial symptoms among the 21 patients with severe disease, CT scan will offer an opportunity to identify patients who are on course of developing severe disease early.

#### 4. Discussion

Our results suggested that a CT scan can be performed as early as 5 days after the initial onset of symptoms, which was prior to patients' symptoms being classified as severe in 18 (85.7%) of the 21 patients. VR thresholds of 11.9% after 5 days and 16.2% after 8 days can be used to identify patients who are on the trajectory to develop severe disease. Although a CT scan on the 8th day can be used to provide even better identification of patients with severe disease, this may limit the usefulness of CT as 10 (47.6%) of the 21 patients already presented with severe symptoms by the 8th day. Future analyses using generalized linear mixed models or other nonlinear longitudinal data analysis approaches of a sufficiently powered study will be needed to further model the progression of VR.

In the United States, CT has not been recommended in the evaluation of COVID-19, especially in the early phase of disease.<sup>2</sup> This recommendation primarily relates to its use for diagnostic purposes, and does not consider the prognostic value. CT imaging might have in the early phase of the disease where triaging of patients who are prone to develop severe disease would be extremely useful. A previous study has found that quantitative CT features outperform the traditional clinical biomarkers including APACHE-II, neutrophil-to-lymphocyte ratio (NLR), and d-dimer levels on early prediction to severe illness in COVID-19 patients. They also found that changes in CT features from day 0 to day 4 performed the best in the prediction than CT features on day 0 and day 4,<sup>14</sup> which is in line with our findings. Another study showed that CT severity score is associated with inflammatory levels and that older age, higher neutrophil-to-lymphocyte ratio (NLR), and CT severity score on

admission are independent risk factors for short-term progression.<sup>15</sup>

The relationship and impact of comorbidities on the severity of COVID-19 had been examined in previous studies,<sup>16–20</sup> and pre-existing conditions such as cancer, chronic kidney disease, COPD, diabetes, cardiovascular disease, and coronary heart disease are known risk factors for increased severity of COVID-19.<sup>21,22</sup> Despite a higher prevalence of cancers, hypertension, diabetes, hyperlipidemia and pulmonary disease in the severe group compared with the non-severe group, none of these differences reached statistical significance in our study, likely due to the limited sample size.

In our study, we evaluated the evolution of CT findings from the onset of symptoms. We classified disease based on extent of symptoms as either severe or non-severe. We were also able to classify disease course into two phases based on the direction of VR change, progressive and recovery phases. We were able to demonstrate a significant difference between the severe and non-severe groups. In the progressive phase, the severe group had both a significantly higher VR (12.0% versus 1.3%) and RAR (2.1% vs. 0.4%) (Figs. 3–4). The capability of quantitative CT imaging to show differences between patients of different clinical severity has previously been demonstrated,<sup>23,24</sup> although it did not attempt to demonstrate the time when differentiation between groups could be made.

Differences of opinion exist between expert societies from different countries in regard to the use of CT for the initial diagnosis of COVID-19, with the US and most European countries recommending against its use except under special circumstances. Our results provide for a new role in its use. The ability to predict early in the course of documented symptomatic disease whether a person will progress to severe disease or be more likely to remain having non-severe would be extremely beneficial in terms of treatment planning allowing for triaging of patients either towards earlier release from the hospital or to be prepared for more intense treatment. This type of evaluation will be especially useful when there is a high volume of cases and hospital resources are being stressed due to high volumes of patients. Our results show that an initial CT scan 5 days following onset of symptoms would allow for confident separation of the two groups. If the results remained in the borderline range or concern still remained, an additional scan 3–4 days later at 8–9 days

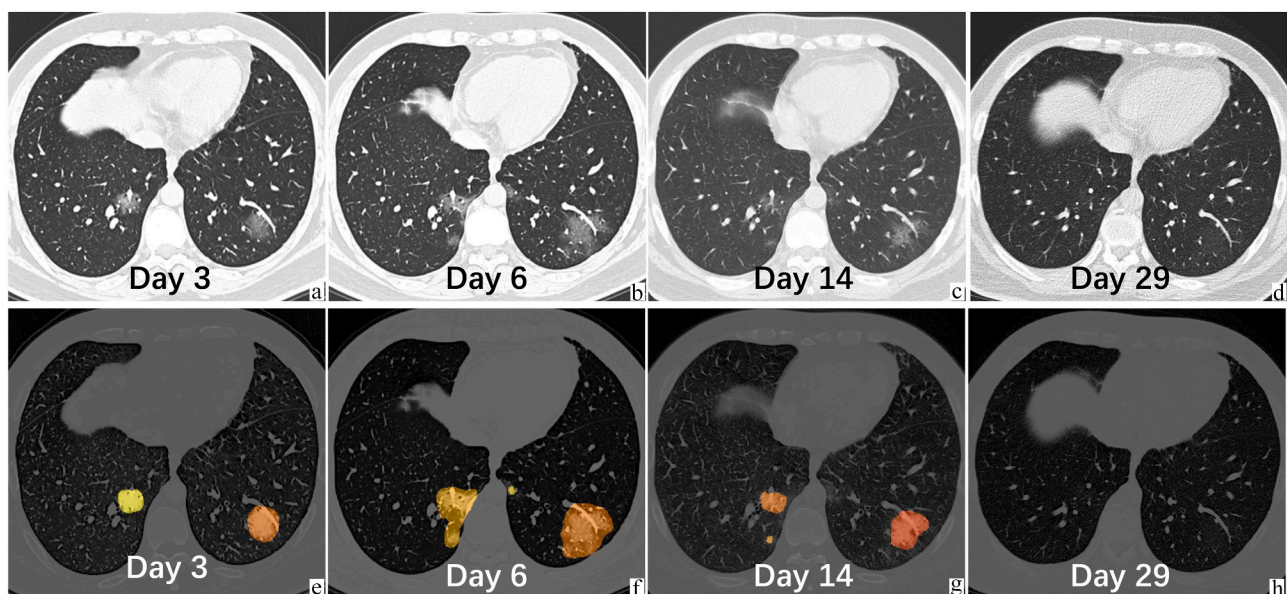


**Fig. 3.** A 29-year-old male, healthy nonsmoker patient with COVID-19 in the non-severe group, who was admitted to the hospital on Feb 1, 3 days after fever with a body temperature of 39 °C. The leukocyte and lymphocyte counts were normal. He was living in Wuhan and traveled to Zhuhai on Jan 23. Original serial chest CT (images a–d, the upper panel) on Feb 1, Feb 4, Feb 12, and Feb 27 demonstrated the evolution of GGO in both lower lobes. The VR was 2.3%, 5.0%, 1.2%, and 0.01%, respectively. The RAR at progressive phase was 0.92% per day. The latter panel (images e–h) displays the segmentation contours based on deep learning algorithm. Different color indicated different lesions. The results have been confirmed by radiologist (KL). This patient was in the progressive phase (a–b), at peak (b), in the recovery phase (b–c), and normal (d).

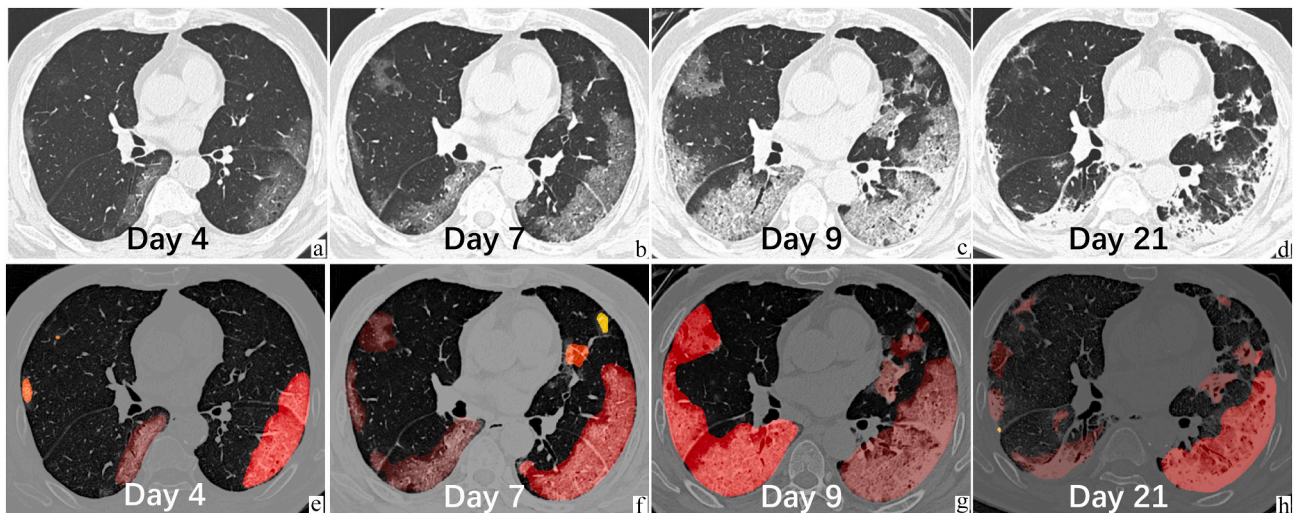


**Fig. 4.** A 69-year-old male in the severe group, with tuberculosis and diabetes, was admitted to the hospital on Jan 23, 3 days after fever with a body temperature of 38.1 °C and developed severe symptoms on the 9th day from onset. The leukocyte and lymphocyte counts were normal. He was living in Wuhan and came to Zhuhai on Jan 19 for Chinese New Year. Original serial chest CT (images a–d, upper panel) on Jan 24, Jan 27, Jan 29, and Feb 10 demonstrated the evolution of bilateral GGOs and consolidation. The VR was 8.3%, 27.4%, 55.6%, and 21.2%, respectively. The RAR at progressive phase was 8.8% per day. The lower panel (images e–h) showed the segmentation contours, with different color representing different lesions. The results were confirmed by radiologist (KL). This patient experienced progressive (a–b, b–c), peak (c), recovery (c–d) phase.

where a repeat VR could be measured and the RAR calculated would add to the confidence as to whether the clinical course would be expected to be severe.

This study is limited by the relatively small number of patients and limited number of CT scans (74 patients with 305 CT scans). Nevertheless, we were able to demonstrate significant differences in the early CT findings that were predictive of the severity of illness. An increase in sample size will further improve the predictive power as well as allow us to consider other potential risk factors such as comorbidities into our model. There were also four cases that ultimately developed severe symptoms that could not be identified on the CT scan on 5th or even the 8th day. However, for triaging purposes we can expect some limitations and we believe it would also be useful to further incorporate additional clinical and laboratory parameters into a more comprehensive model. Our results also relied on a specific CT scanner and previously validated AI software. However, our results were reviewed by two radiologists to confirm that the software performed appropriately and therefore any major errors would have been detected. Since we are looking for fairly large effects, it is unlikely that different software would have substantially changed our results. While our results are limited to the use of a single software, the development of new software specifically for the purpose used here is already underway by multiple manufacturers and the academic community at large. This has culminated in the organization of an open source databases that has been sponsored by multiple organizations to specifically be used for development of this type of software.<sup>25</sup> While it is likely that different software will have some variation, the overall magnitude of the changes found here, and the agreement of radiologists regarding its performance strongly supports that there will be an overall role for automated software specifically for this purpose. In cases where the AI algorithm failed to identify lesions and provide VR estimates, visual estimation of the overall volume was done by radiologist. While this was only an estimate, it likely did not substantially alter the overall score as the lesions that the software missed were typically small and subtle and contributed little to the overall score and only occurred in a small 8.5% (26/305) of CT scans. An additional limitation relates to our only having a limited number of CT scans on each individual and therefore we do not know for sure what time the actual time and the extent of maximum CT abnormalities occurred. We are only able to look at the whole group and estimate this. As additional cases accumulate it is likely that our ability to make better

predictions will improve. Finally, as repeated CT examinations may be performed on a subgroup of patients, radiation dose of the CT scans should be minimized to the lowest amount while maintaining image quality.<sup>9</sup>

In summary, our data suggest a strong rationale for performing CT in the context of a known diagnosis of COVID-19 where it can be used for prognostic purposes. This approach allows for better triaging of patients to optimal management pathways. Under these circumstances, especially when the prevalence of disease in the community is high and therefore where the pretest probability of lung disease being related to COVID is also high, concerns for competing differential diagnosis are minimized. As guidelines have continued to evolve regarding how to improve safety within radiology departments obtaining scans on COVID-19 patients, it may allow for increased use of CT scanning when the prognostic information provided by its use is considered especially meaningful. Our results await confirmation with additional larger datasets as well as further refinements of imaging parameters and incorporation of laboratory values into a more comprehensive predictive model.

#### Declaration of competing interest

Authors declare that everyone has no conflict of interest.

#### Acknowledgments

We thank the team from HY Medical Technology for their technical assistance in use of the deep learning-based algorithm.

We kindly request a waiver of IRB consent for our retrospective study on Early Prediction of Severity in Coronavirus Disease (COVID-19) using Quantitative CT Imaging. Study participation presents no risk of harm to the subject, and the research involves no procedures. The principal risk is potential harm resulting from a breach of confidentiality, but there is no record linking the subject and the research. In addition, this work is designated to study, evaluate, and provide for public benefit.

## References

1. WHO Director-general's opening remarks at media briefing on COVID-19. <https://www.who.int/dg/speeches/detail/who-director-general-s-opening-remarks-at-the-media-briefing-on-covid-19-11-march-2020>. [Accessed 3 April 2020].
2. ACR recommendations for the use of chest radiography and computed tomography (CT) for suspected COVID-19 infection. <https://www.acr.org/Advocacy-and-Economics/ACR-Position-Statements/Recommendations-for-Chest-Radiography-and-CT-for-Suspected-COVID19-Infection>. [Accessed 3 April 2020].
- [3] Hope M, Raptis C, Shah A, et al. A role for CT in COVID-19? What data really tell us so far. *Lancet* Mar 27 2020. [https://doi.org/10.1016/S0140-6736\(20\)30728-5](https://doi.org/10.1016/S0140-6736(20)30728-5) [pii: S0140-6736(20)30728-5, Epub ahead of print].
4. Chinese Society of Radiology. Imaging diagnosis of 2019-nCoV pneumonia: expert recommendation of Chinese Society of Radiology, the first edition. *Chin J Radiol* 2020;54(00):E001. <https://doi.org/10.3760/cma.j.issn.1005-1201.2020.0001>.
- [5] Chung M, Bernheim A, Mei X, et al. CT imaging features of 2019 novel coronavirus (2019-nCoV). *Radiology* 2020;295(1):202–7. <https://doi.org/10.1148/radiol.2020200230>.
- [6] Simpson S, Kay F, Abbara S, et al. Radiological Society of North America expert consensus statement on reporting chest CT findings related to COVID-19. Endorsed by the Society of Thoracic Radiology, the American College of Radiology, and RSNA. *Radiol Cardiothorac Imaging* Mar 25 2020. <https://doi.org/10.1148/ryct.2020200152> [published online].
- [7] Pan F, Ye T, Sun P, et al. Time course of lung changes on chest CT during recovery from 2019 novel coronavirus (COVID-19) pneumonia. *Radiology* Feb 13 2020: 200370. <https://doi.org/10.1148/radiol.2020200370> [Epub ahead of print].
- [8] Bernheim A, Mei X, Huang M, et al. Chest CT findings in coronavirus disease-19 (COVID-19): relationship to duration of infection. *Radiology* Feb 20 2020:200463. <https://doi.org/10.1148/radiol.2020200463> [Epub ahead of print].
- [9] Kwee TC, Kwee RM. Chest CT in COVID-19: what the radiologist needs to know. *Radiographics* Nov–Dec 2020;40(7):1848–65. <https://doi.org/10.1148/rg.2020200159> [Epub 2020 Oct 23. PMID: 33095680; PMCID: PMC7587296].
10. National Health Commission of the People's Republic of China. Diagnosis and treatment of pneumonia caused by novel coronavirus infection (trial version 7 revised version) [EB/OL].2020-03-04. <http://www.nhc.gov.cn/zycj/s7653p/202003/46c9294a7dfe4cef80dc7f5912eb1989.shtml>.
- [11] Li K, Fang Y, Li W, et al. CT image visual quantitative evaluation and clinical classification of corona virus disease (COVID-19). *Eur Radiol* 2020. <https://doi.org/10.1007/s00330-020-06817-6>.
- [12] Sun K, Xiao B, Liu D, Wang J. Deep high-resolution representation learning for human pose estimation. In: *Proceedings of the IEEE Conference on Computer Vision and Pattern Recognition*; 2019. p. 5693–703.
13. Sun K, Zhao Y, Jiang B, et al. High-resolution representations for labeling pixels and regions. *arXiv:1904.04514*, 2019.
- [14] Liu F, Zhang Q, Huang C, et al. CT quantification of pneumonia lesions in early days predicts progression to severe illness in a cohort of COVID-19 patients. *Theranostics* 2020;10(12):5613–22.
15. Feng Z, Yu Q, Yao S, et al. Early prediction of disease progression in COVID-19 pneumonia patients with chest CT and clinical characteristics. *Nat Commun*.
- [16] Luo, et al. The potential association between common comorbidities and severity and mortality of coronavirus disease 2019: a pooled analysis. *Clin Cardio* 2020 Dec;43(12):1478–93.
- [17] Miller LE, et al. Diabetes mellitus increases the risk of hospital mortality in patients with COVID-19: systematic review with meta-analysis. *Medicine (Baltimore)* 2020 Oct 2;99(40):e22439.
18. Sanyaolu, et al. Comorbidity and its impact on patients with COVID-19. *SN Compr Clin Med* 2020 Jun 25:1–8.
19. Romagnolo, et al. Neurological comorbidity and severity of COVID-19. *J Neurol* 2021 Mar;268(3):762–9.
20. Richardson, et al. Presenting characteristics, comorbidities, and outcomes among 5700 patients hospitalized with COVID-19 in the NYC area. *JAMA* 2020 May 26;323(20):2052–9.
21. Coronavirus Disease 2019 (COVID-19). Who is at increased risk for severe illness? - people of any age with underlying medical conditions [Ctr Dis Control Prev]. Available at: <http://www.cdc.gov/coronavirus/2019-ncov/need-extra-precautions/people-with-medical-conditions.html>. [Accessed 23 November 2020].
22. Coronavirus Disease 2019 (COVID-19). Evidence used to update the list of underlying medical conditions that increase a person's risk of severe illness from COVID-19, Centers for Disease Control and Prevention. . Available at: <http://www.cdc.gov/coronavirus/2019-ncov/need-extra-precautions/evidence-table.html>. [Accessed 23 November 2020].
- [23] Jiang X, Coffee M, Bari A, et al. Towards an artificial intelligence framework for data-driven prediction of coronavirus clinical severity. *Computers, Materials & Continua* 2020;63:537–51.
- [24] Huang L, Han R, Ai T, et al. Serial quantitative chest CT assessment of COVID-19: deep-learning approach. *Radiol Cardiothorac Imaging* 2020;2(2). <https://doi.org/10.1148/ryct.2020200075>.
25. NIH harnesses AI for COVID-19 diagnosis, treatment, and monitoring, NIH News Release. <https://www.nih.gov/news-events/news-releases/nih-harnesses-ai-covid-19-diagnosis-treatment-monitoring>.